

Synthesis and Characterization of MEH-PPV for Solar Cell Application

F.A. Mahmoud^{1,2*}, Y. Assem^{2,3**}, A.B. Shehata⁴, D.E. Motaung⁵

¹Solid State Physics Dept., ²Solar Cell Lab., Center of Excellence for Advanced Sciences, ³Polymer and Pigments Dept., National Research Centre, 33 Elbuhouth st., Dokki, Giza, 12622. ⁴National Institute of Standards, Tersa St. El Haram, Giza P.O. 136 Giza, code 12211, Egypt and ⁵DST/CSIR National Centre for Nano-structured Materials, Council for Scientific Industrial Research, Pretoria, 0001, South Africa.

POLY [2- methoxy -5 -(2'- ethylhexyloxy) - (p - phenylenevinylene)] (MEH-PPV) was prepared via Gilch route. The structures of MEH-PPV were fully confirmed with their respective spectroscopic data using ¹H and ¹³C nuclear magnetic resonance (NMR) and Fourier transform infrared (FTIR) spectroscopies. Thermal properties of the polymer were studied using simultaneous Thermo-Gravimetric and Differential Scanning Calorimetry (TGA/DSC) analyses. The number average molecular weight M_n of the prepared MEH-PPV was measured by Gel permeation chromatography (GPC) technique. To investigate the physical properties of the prepared MEH-PPV, two polymer samples were dissolved in two different organic solvents (THF and Chlorobenzene CB) and sprayed as a film on top of the glass and KBr substrates at 150 °C. The dissolved MEH-PPV polymer in THF was sprayed onto ZnO nanowires that grown on FTO glass substrate by two step method. The constructed solar cell showed better performance compared with previous cell that based on sprayed MEH-PPV / sprayed ZnO nanorod/TCO glass

Keywords: Solar cell, MEH-PPV, Nanowires, Thin films and Nanorods.

Poly [2-methoxy-5-(2'-ethylhexyloxy)-1,4-phenylene vinylene] (MEH-PPV) is an electroluminescent polymer, widely utilized in the fabrication of Polymer Light Emitting Diodes (PLEDs). The application of this polymer is mainly focused on display such as Light Emitting Diode (LEDs), field effect transistor and photovoltaic cells⁽¹⁾. Recent studies on the material have shown that the polymer morphology, as well as the polymer processing conditions such as the type of solvent spin coating speed, solution concentration and annealing temperature, are important factors in determining the final physical properties of the polymer thin films and subsequently the performance of the device made from the polymer⁽²⁾. MEH-PPV is one of the derivatives with alkoxy on phenyl groups⁽³⁾ and exhibits

*Email: fa.mahmoud@nrc.sci.eg , fawzyhameed@yahoo.com

**Email: ya.assem@nrc.sci.eg ammar_abu2002@yahoo.com

superior solubility in common organic solvents such as tetrahydrofuran (THF), chloroform, xylene, chlorobenzene (CB) and toluene. It can form a solution at room temperature and turned into a uniform thin film with a large area and could display good optical properties⁽⁴⁾. This film could be produced by either spin coating or spray coating techniques. Spray coating technique is one of the easiest techniques to produce uniform films onto a large area.

Solar cells based on nanostructured materials have recently attracted considerable interest as they improve optical light trapping, offer enhanced interface areas for carrier separation, and very simple fabrication procedures^[5, 6]. Incorporation of nanowires into this type of solar cell holds promise to improve the charge carrier transport for at least one carrier type. Molecular dye layers, polymers and ultrathin inorganic semiconductor layers have been considered as suitable absorber materials for these cells⁽⁷⁻¹²⁾. Herein, we report on a preparation of MEH-PPV polymer using the Gilch route. We also report on a new solar cell structure which uses MEH-PPV as the precursor for the optically active absorber material. Two thin layers based on MEH-PPV polymer were examined; the two layers were sprayed from either THF or CB. The absorber polymeric layer that dissolved in THF is deposited on n-type ZnO nanowires, which provide a fast electron pathway to the SnO₂:F substrate. The polymer layers deposition processes are carried out at temperatures below 150°C. The constructed solar cell is characterized and its efficiency is compared with that published from our previous results that have the same structure but replaces ZnO nanowires by sprayed ZnO nanorods⁽⁶⁾.

Materials and Methods

P-methoxyphenol(99% purity), tetrabutylammonium bromide(98 % purity), 2-ethylhexyl bromide 95%, paraformaldehyde (reagent grade), acetic acid(99 % purity), HBr (48 %purity),ACS grade, all were purchased from Sigma-Aldrich and used as received, all solvents are distilled before use, and dried over sodium metal if necessary.

Synthesis of MEH-PPV

Synthesis of Methoxy-4-(2-ethylhexyloxy) benzene) (A)

P-methoxyphenol (100 g, 0.81 mol), KOH (56 g, 1 mol), tetrabutylammonium bromide (5 g, 0.17 mol), and water (300 ml) were added to a round-bottom flask. Subsequently, 154 g of 2-ethylhexyl bromide was added to the mixture and refluxed at 70 °C for 72 hr under N₂ atmosphere. After cooling the mixture to room temperature, the organic layer was extracted with ether and subjected to rotary evaporator to remove the solvent. The obtained brown liquid was distilled under reduced pressure to obtain a yellow liquid of 1-methoxy-4-(2-ethylhexyloxy) benzene, 80 %.

Synthesis of α,α' -Dibromo-2-methoxy-5-(2-ethylhexyloxy)xylene(B)

50 g Methoxy-4-(2-ethylhexyloxy) benzene, 30 g paraformaldehyde, and 100 ml acetic acid, along with 100 mL HBr, were mixed in a round-bottom flask equipped with magnet bar and left to react in an oil bath at 70 °C for 4 hr under nitrogen atmosphere. At the end of the reaction, the product was cooled to room temperature. A solid mass was obtained, diluted with chloroform and washed with saturated solution of sodium bicarbonate, at least, two times. The organic layer was separated and dried over anhydrous magnesium sulphate (MgSO₄) followed by removal of chloroform. The crude product was recrystallized from n-hexane dried in vacuum to get a solid powder of α,α' -dibromo-2-methoxy-5-(2-ethylhexyloxy)xylene with a yield of 81%.

Polymerizations of α,α' -Dibromo-2-methoxy-5-(2-ethylhexyloxy)xylene

The polymerization was carried out in dry dioxin, where 1.5 g of tert-butylbutoxide was added to 100 ml dry dioxane in a round bottom two-neck flask equipped with a condenser. The solution was purged with N₂ for 30 min. After that, the reaction temperature was elevated to 50 °C. A solution of B (2 g) in 30 ml dry dioxane was added dropwise to the reaction solution via dropping funnel for about 20 min under N₂ gas. The reaction was continued for 8 h. and the reaction mixture turned orange. At the end of the reaction, the obtained polymer was dissolved in THF and filtered to get rid of the gel content. The filtrate was concentrated and precipitated in methanol to obtain a reddish- orange solid of MEH-PPV 63%.

The structure of prepared purified polymer MEH-PPV fully was comply with their respective spectroscopic data using ¹HNMR and FTIR spectroscopy. The thermal properties of the polymer were studied using simultaneous thermogravimetry and differential scanning Calorimetry (TGA/DSC) techniques. Also, the number average molecular weight M_n of the prepared MEH-PPV was measured by Gel permeation chromatography (GPC) technique. The basic optical properties of MEH-PPV have been extensively studied, however; the photoluminescence measurements on MEH-PPV were examined.

ZnO nanowires preparation

The ZnO nanowires array was prepared using two-step chemical solution method. Firstly, 0.3 M zinc acetate dihydrate was dissolved in ethanol. For total dissolution, equal molar amount of diethanolamine was added slowly to the solution. The resultant solution was stirred 30 min to yield a clear transparent homogeneous solution. Then the solution was subjected to spin coating on patterned cleaned fluorine tin oxide (FTO)-coated glass substrates. The sample was annealed for 1 hr in air to obtain ZnO nanoparticles seed layer. Secondly, ZnO nanowires were grown on the ZnO seeded-substrates by immersing them in a closed vial containing zinc nitrate hexahydrate and hexamethylenetetramine (HMT) in deionized water at 100 °C for 8 hr. Subsequently, the substrates were rinsed thoroughly with distilled water to remove any residual reactants and dried in air for 1 hr.

Polymer film preparation

After preparation of MEH-PPV polymer, two specimens were dissolved in two different organic solvents, chlorobenzene and THF, to prepare two series from sprayed MEH-PPV thin film, on glass and KBr substrates preheated at 150°C using nitrogen as a carrier gas. The structure and optical properties of prepared films were investigated by FTIR, Photoluminescence and UV-VIS-NIR spectroscopy. Surface morphology was examined using a JOEL scanning electron microscope (Oxford instruments INCA-Sight 40KV). The D.C. electrical properties were measured by Lakeshore 7700A Hall effect system. To test our polymer as an active layer for organic-inorganic solar cell, the best polymer film based on the type of the solvent was deposited onto the ZnO nanowires layer that was prepared by two steps method onto the FTO glass substrate. Current density–voltage (J–V) measurements of the constructed solar cell were characterized using a Keithley 4200 source measurement unit (Keithley, USA) under simulated 100 mW/cm² (AM 1.5 G) irradiation from a Newport solar simulator and the cell efficiency was calculated and compared with the efficiency of our previous solar cell⁽⁶⁾, that have the same structure, but replaces ZnO nanowires by sprayed ZnO nanorods.

Characterization

Nuclear magnetic resonance spectroscopy (NMR)

¹H and ¹³C NMR spectra were recorded on JEOL ECA-500 run at 500 MHz. The monomer and polymer specimens were dissolved in CDCl₃, and tetramethylsilane was used as the reference standard.

Gel permeation chromatography (GPC)

The molecular weights of the prepared polymer were measured by Chloroform GPC at 25°C. Sample concentration was 1 g L⁻¹. The apparatus consists of a Gynkotek HPLC pump, an Agilent Autosampler 1200, linear columns (PSS, polystyrene) consisting of a pre-column 10 μ, 8 x 50 mm, a column 10 Å, 8 x 300 mm and two columns 3000 Å, 8 x 300 mm. As a detector, RI detector of Knauer Company was used. Linear PMMA with a narrow mass distribution and a molecular weight between 500 and 1,000,000 were used to set up a calibration plot. Toluene was used as an internal standard. The elugram was evaluated with PSS WinGPC Unity program.

Fourier Transform Infrared spectroscopy (FTIR)

The IR spectra were measured on a FT-IR spectrometer of type Excalibur Series with an attached Infrared spectroscopy (IR) microscope of the type UMA 600 from Digilab. IR measurements were performed by means of Digilab (Excalibur series) instrument with ATR crystal ZnSe and WinIRPro software version 3.3.

Thermal Gravimetric Analysis (TGA)

Thermal stability was determined by recording TGA traces in a nitrogen atmosphere (flow rate = 50 mL min⁻¹) using a TA Q500 thermogravimetric analyser. A heating rate of 10°C min⁻¹ and a sample size of 10-12 mg was used

Egypt. J. Chem. **59**, No. 5 (2016)

in each experiment. The sample was heated from room temperature to 800 °C at a heating rate of 10 °C/min.

Differential Scanning Calorimetry (DSC)

Mettler Thermal Analyzer having 821 DSC module was used for thermal analysis of the polymer. Prior to measurements, approximately 10 mg of the sample was loaded in an aluminium pan. DSC scans were recorded in a nitrogen atmosphere (flow rate = 80 ml min⁻¹), the sample was heated in the first heating cycle from -100 °C to 100 °C at a heating rate of 20 °C/min. The sample was cooled again to -100 °C with a cooling rate of 20 °C/min and heated again in the second cycle upto 100 °C.

Results and Discussion

Polymer part

Poly [2-methoxy-5-(2'-ethylhexyloxy)-1,4-phenylene vinylene] MEH-PPV was synthesized over 3 steps. Firstly, we prepared Methoxy-4-(2-ethylhexyloxy) benzene and prepared α,α' dibromo-2-methoxy-5-(2-ethylhexyloxy) xylene and finally using Gilch route to obtain the target polymer MEH-PPV as schemed in Fig. 1^(13,14). The solid polymer is also shown in Fig. 2.

Structural properties

¹HNMR and ¹³CNMR spectra of Methoxy-4-(2-ethylhexyloxy) benzene (A) and α,α' -Dibromo-2-methoxy-5-(2-ethylhexyloxy)xylene (B) are shown in Fig. 3-6. The peaks are assigned leisurely according to the literature^(13,14). For Methoxy-4-(2-ethylhexyloxy) benzene, the five aromatic protons are assigned at 6.8 ppm, 15 aliphatic protons are assigned at 0.9-1.7 ppm while the five methoxy protons are assigned at 3.7 ppm as shown in Fig. 3. In Fig. 4, the ¹³C NMR spectrum of Methoxy-4-(2-ethylhexyloxy) benzene is also assigned, where the 2 aromatic carbon atoms attached to oxygen are assigned at 153.6 and 153.9 ppm, the other four are assigned at 114-115 ppm. The 2 carbons attached to methoxy oxygen (No. 1 and 10 Fig. 4) are assigned at 71.2 and 55.8 ppm. Finally, seven aliphatic carbons of the ethyl hexyl moiety are assigned at 11-40 ppm as shown in Fig. 4. For α,α' -Dibromo-2-methoxy-5-(2-ethylhexyloxy) xylene, it is noted that an extra peak appeared at 4.5 ppm that corresponds to the four methylene protons attached to two bromine atoms as shown in Fig. 5, while the carbon atoms of these two methylene groups are assigned at 28.5 and 28.6 ppm, as shown in Fig. 6. The ¹HNMR spectrum of purified MEH-PPV is shown in Fig. 7, where the peak of methylene protons at 4.5 ppm disappeared and an extra peak of the vinyl protons appeared at 6.375-7.25 ppm. Also, the two aromatic protons are assigned at 7.5 ppm. The aliphatic and the methoxy protons are assigned as in the monomers.⁽¹⁴⁻¹⁶⁾

For identifying the molecular components and structures, the FTIR measurements for polymers were carried out to confirm the hydrogen-bonding assembly process. Figure 8 shows the FTIR spectrum of the MEH-PPV polymer. The bands at 703 and 768 cm⁻¹ are referred to the monosubstituted aromatic ring C-H bending. The vibration band at 964 cm⁻¹ is ascribed to the vinylene CH

wag, and is to probe the conjugation of the polymer. The other vibrations observed at 857 cm^{-1} , 1374 cm^{-1} , 1462 cm^{-1} are related to out-of-plane phenyl-CH wag, symmetric alkyl CH_2 , and asymmetric alkyl CH_2 , respectively. Three semicircular stretch bands associated with the phenyl ring are observed at 1412 , 1501 , and 1598 cm^{-1} . The two absorption bands associated with C–O single bonds, the band at 1204 cm^{-1} related to the phenyl-oxygen stretch was the strongest absorption band, and the band at 1038 cm^{-1} was due to the alkyl-oxygen stretch. The bands at 1250 and 1312 cm^{-1} arose from the ether C–O stretch. Absorption bands at 2856 , 2910 , 2956 , and 3057 cm^{-1} were CH_2 , CH , asymmetric CH_3 , and aromatic CH stretch, respectively ⁽⁶⁾.

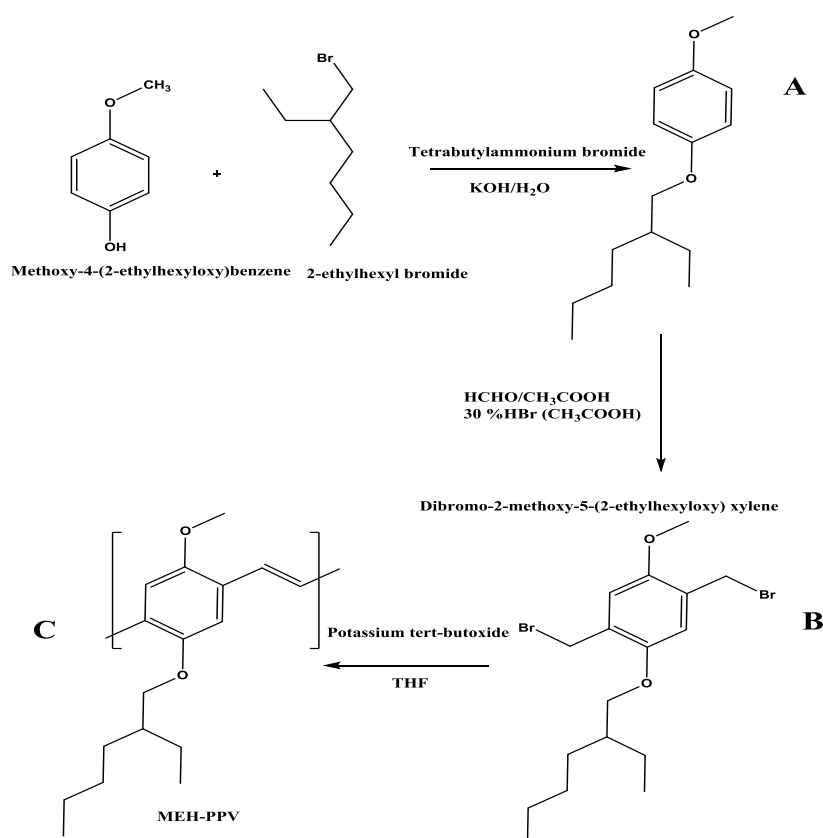
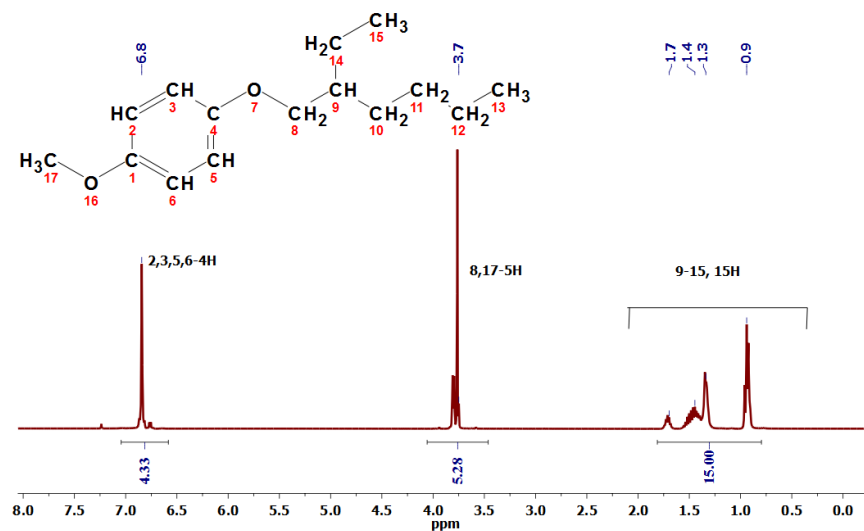
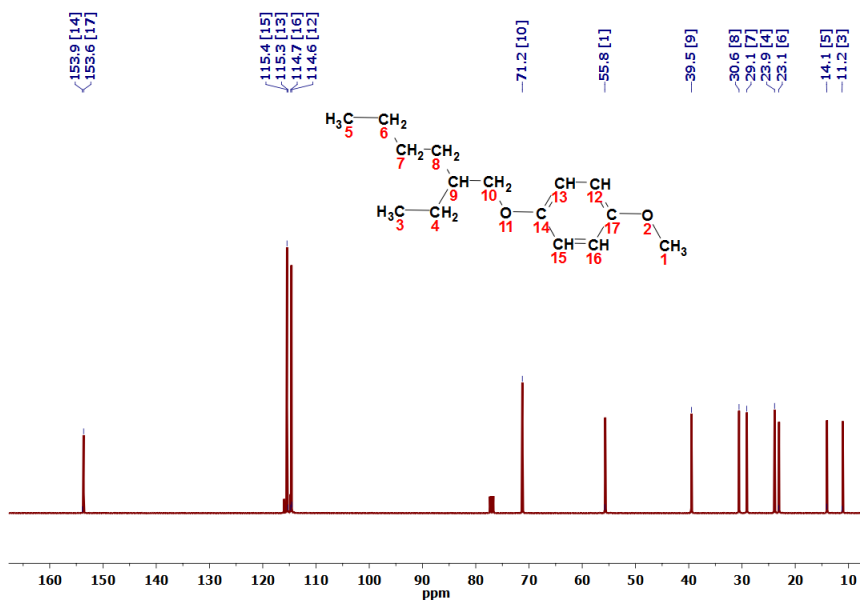


Fig. 1. Schematic diagram showing the synthesis process of MEH-PPV.



Fig. 2. Micrograph of the as-prepared MEH-PPV powder.

Fig 3. ^1H NMR of Methoxy-4-(2-ethylhexyloxy) benzene (A).Fig. 4. ^{13}C NMR of Methoxy-4-(2-ethylhexyloxy) benzene.

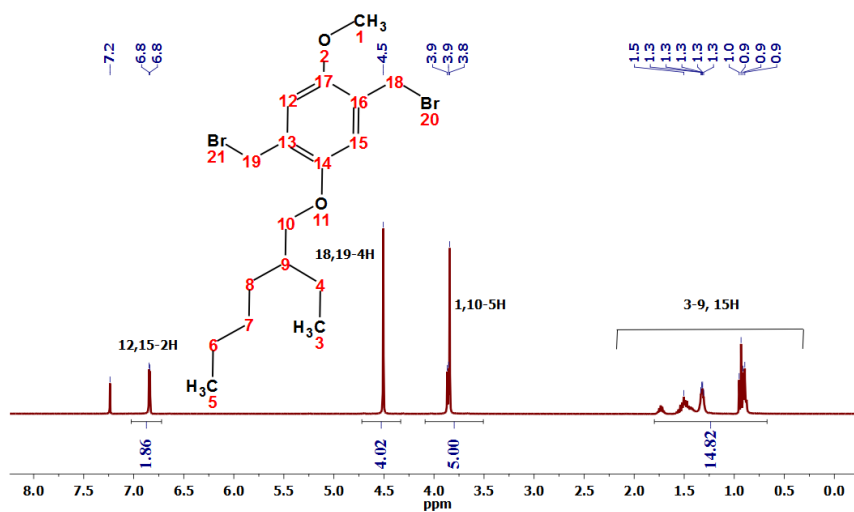


Fig. 5. ¹H NMR of α, α' -Dibromo-2-methoxy-5-(2-ethylhexyloxy)xylene.

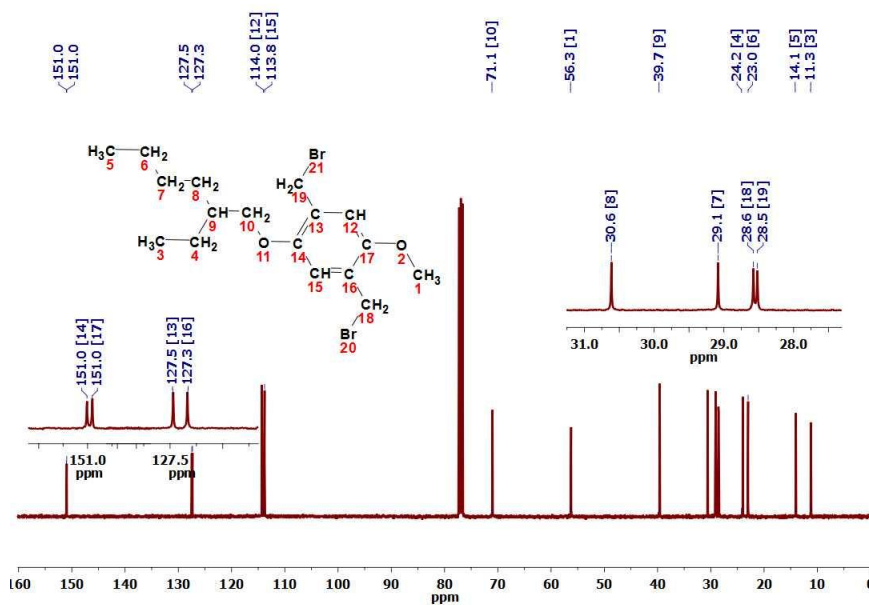


Fig. 6. ¹³C NMR of α, α' -Dibromo-2-methoxy-5-(2-ethylhexyloxy)xylene .

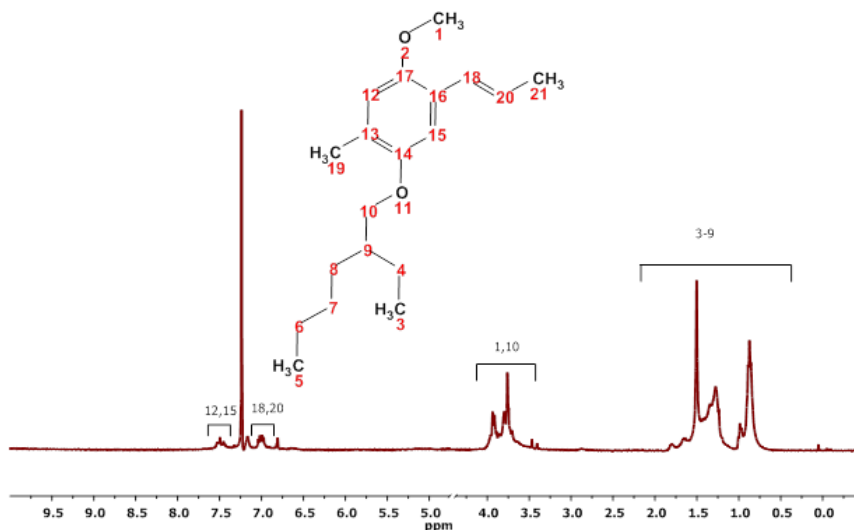


Fig 7. ¹H NMR of MEH-PPV.

The number average molecular weight M_n of the prepared MEH-PPV was measured by Gel permeation chromatography (GPC) technique. We found that the molecular weight of the polymer is broadly distributed and the number average molecular weight (M_n) was found to be 4.26×10^4 g/mol. This high molecular weight indicates a good strength, hardness and thermal stability of the prepared polymer, MEH-PPV.

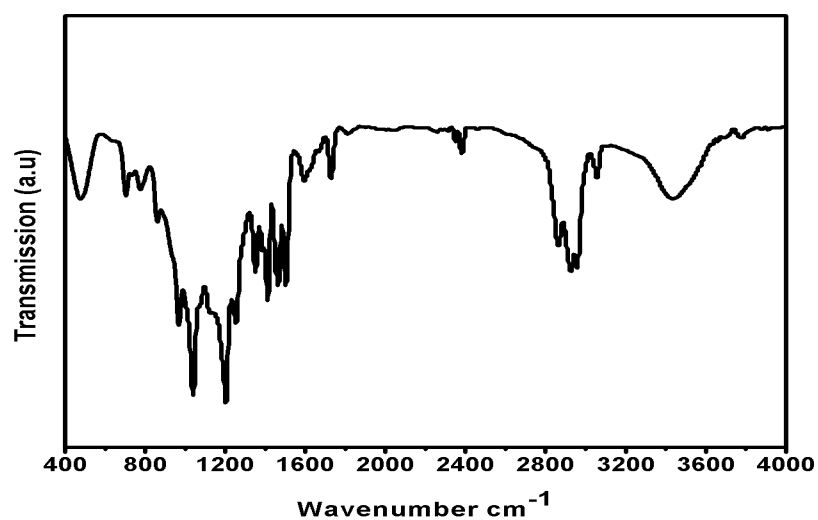


Fig. 8. FTIR spectrum of the MEH-PPV polymer.

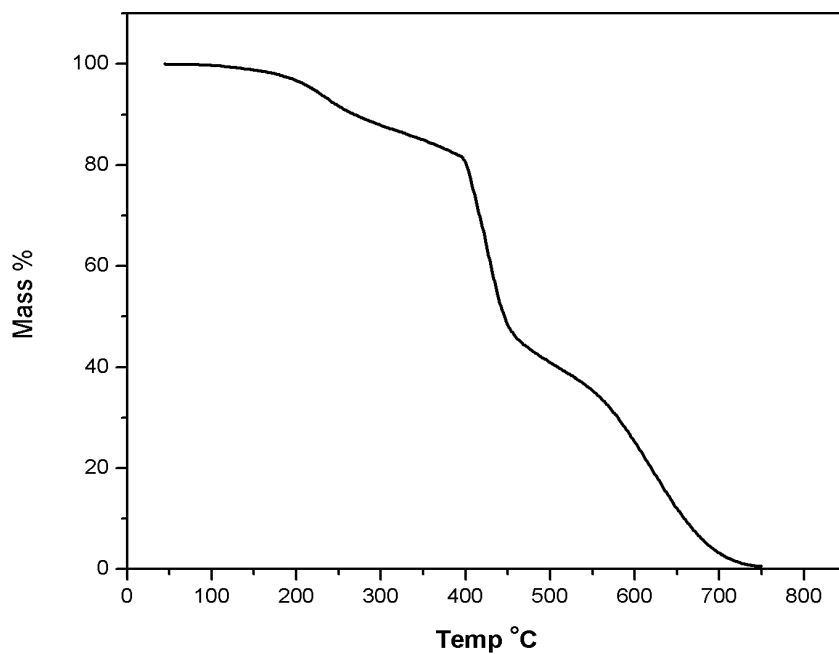


Fig. 9.The DTGA analysis of MEH-PPV powder.

Thermogravimetric analysis (TGA) was performed to characterize the heat decomposition behavior of the prepared MEH-PPV. Approximately 7.04 mg sample of the polymer was heated under nitrogen using TA Q500 thermogravimetric analyser up to 800 °C and the results are presented in Fig.9. It can be seen from the figure that the polymer started decomposition at 150-200 °C related to the removal of physically and chemically adsorbed water molecules. At 400 °C, about 18% weight loss occurred, which may be due to the loss of an alkyl side group attached to the aromatic thiophene backbone. A larger exothermic peak around 400 °C, indicates a good thermal stability for the photovoltaic application. A sharp decomposition was then observed between 400- 450 °C, where the polymer lost about 55 % of its weight. The weight loss continued until full decomposition at about 750°C.

The DSC thermogram of MEH-PPV is shown in Fig. 10. The glass transition temperature, T_g of the sample is found to be around 57 °C. This is lower than what is reported by Liu *et al.* (70 °C)⁽¹⁷⁻¹⁸⁾ and Lee *et al.* (65 °C)⁽¹⁹⁾. However, it is consistent with that reported by Souza *et al.* (57°C)⁽²⁰⁾. In addition, crystallization exothermic peaks (T_{cc}) could be observed at 98 °C in the 2nd cooling cycle.

Optical properties and photoluminescence

In order to investigate the spectral properties of the polymer structures, it is necessary to study the individual absorption properties of the polymer. Figure 11a illustrates the absorption spectrum of the MEH-PPV polymer. The polymer showed almost the same absorption spectra whose λ_{max} is around 482 nm. The absorption edges of the polymer films appear around 580 nm that was used for determining the optical band gap.

The PL spectrum of the polymer is also shown in Fig. 11b. It seems to be composed of three Gaussian curves whose sum is fit to the pristine PL spectrum. Three discernible peaks are obviously resolved to provide information about a single electronic state (0–0 emission band) and the featureless vibronic structures such as 0–1, 0–2 emission bands upon excitation in the solution state [ref]. The pure MEH-PPV polymer is characterized by two main peaks at 592 nm with a much weaker red shoulder at about 636 nm. It is well accepted that the emission peak at 592 nm arises from single-chain excitons (*e.g.* intrachain excitation), while the peak at 698 nm is associated with interchain interactive excimers and is related to aggregation of polymer chains^(21,22).

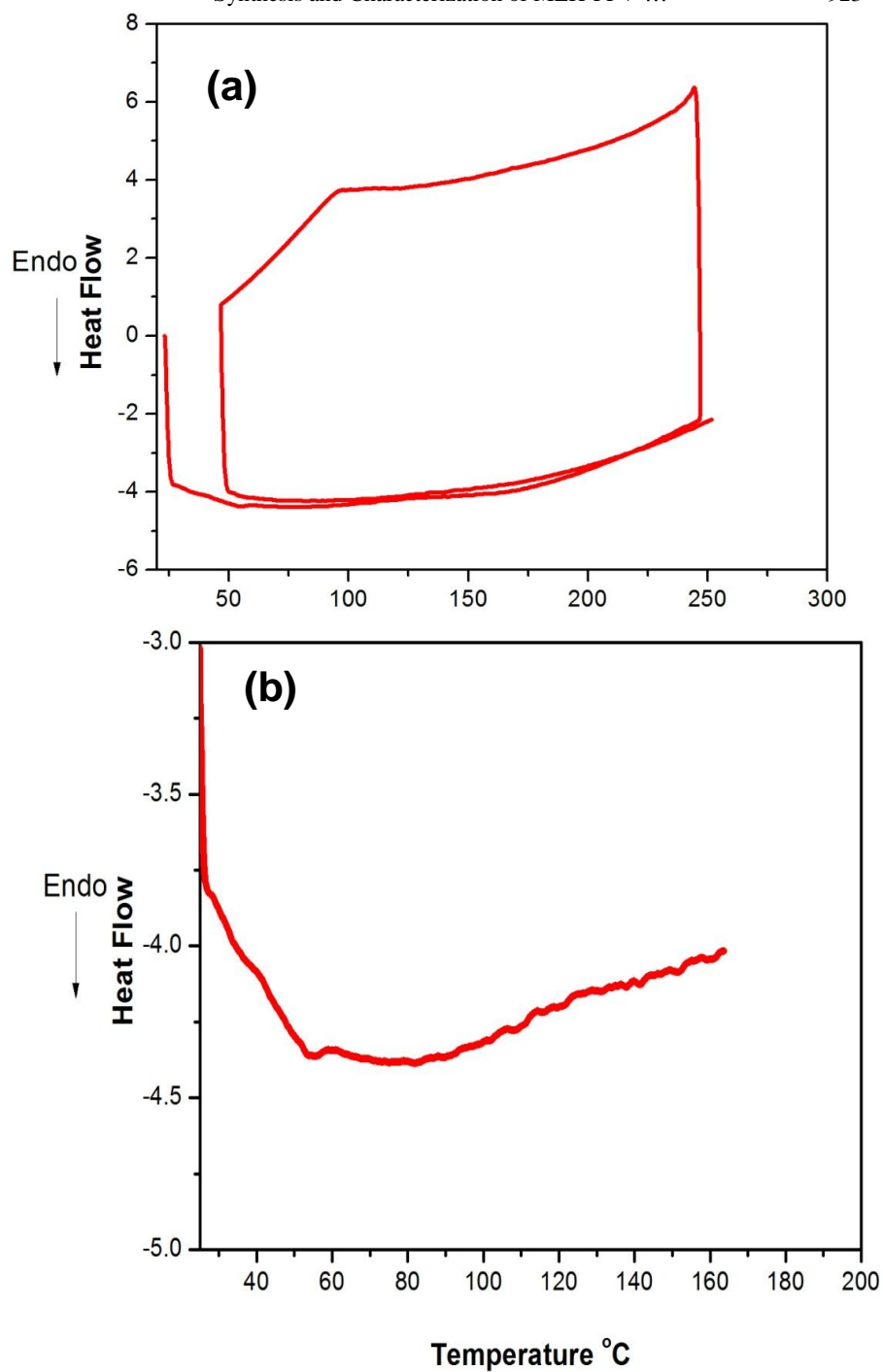


Fig. 10. DSC thermogram of MEH-PPV: whole curve (a) and heating cycle (b).

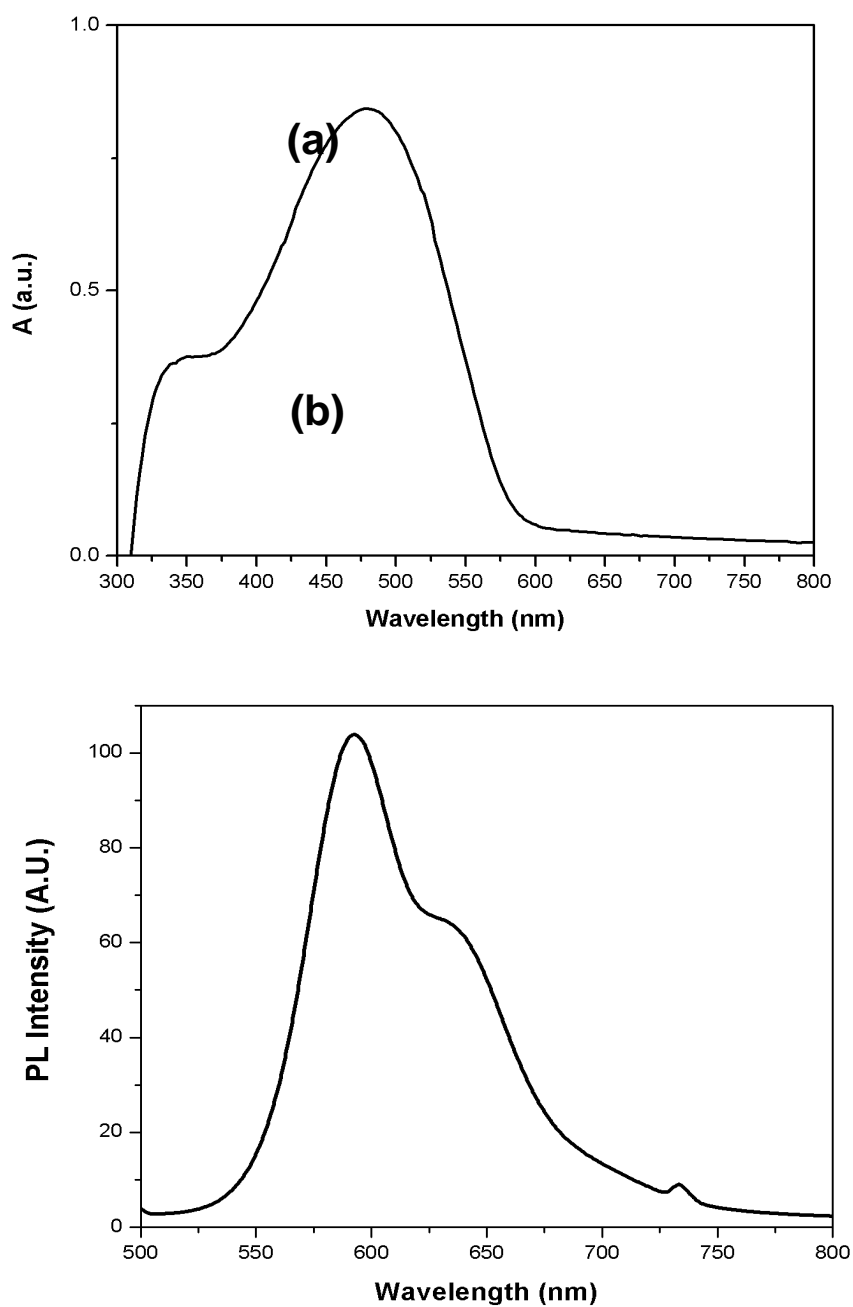


Fig. 11.(a) UV-vis absorption spectrum(b) PL spectrum of the MEH-PPV polymer.

Polymeric thin film

Figure 12 shows the FTIR spectra for different sprayed MEH-PPV films based on the type of the used solvent either THF or CB using N_2 as an atomizing gas. The molecular orientation can be found from the peak of the spectra. The bands at 703 and 768 cm^{-1} referred to the mono-substituted aromatic ring C–H bending. The vibration at 964 cm^{-1} ascribed to the vinylene CH wagging, which verified the conjugation of the polymer. Jie Liu *et al.*⁽¹⁷⁾ have reported that transitions at 850 and 965 cm^{-1} have dipoles normal to the phenyl-vinyl plane. The intensities of the two peaks are expected to be higher when the phenyl-vinyl planes are aligned parallel to the sample surface compared to that when they are aligned perpendicular to the substrate surface. The other vibrations indicative of the MEH-PPV structure were the 857 cm^{-1} out-of-plane phenyl-CH wag, the 1374 cm^{-1} symmetric alkyl CH_2 , and the 1462 cm^{-1} asymmetric alkyl CH_2 . Three semicircular stretch bands associated with the phenyl ring were at 1412 , 1501 , and 1598 cm^{-1} . There were two absorption bands associated with C–O single bonds, the band at 1204 cm^{-1} related to the phenyl-oxygen stretch was the strongest absorption band, and the band at 1038 cm^{-1} was due to the alkyl-oxygen stretch. The bands at 1250 and 1312 cm^{-1} arose from the ether C–O stretch. Absorption bands at 2856 , 2910 , 2956 , and 3057 cm^{-1} were CH_2 , CH, asymmetric CH_3 , and aromatic CH stretch, respectively. The intensity of the transmission peaks is slightly changed for MEH-PPV thin film prepared from two different solvents.

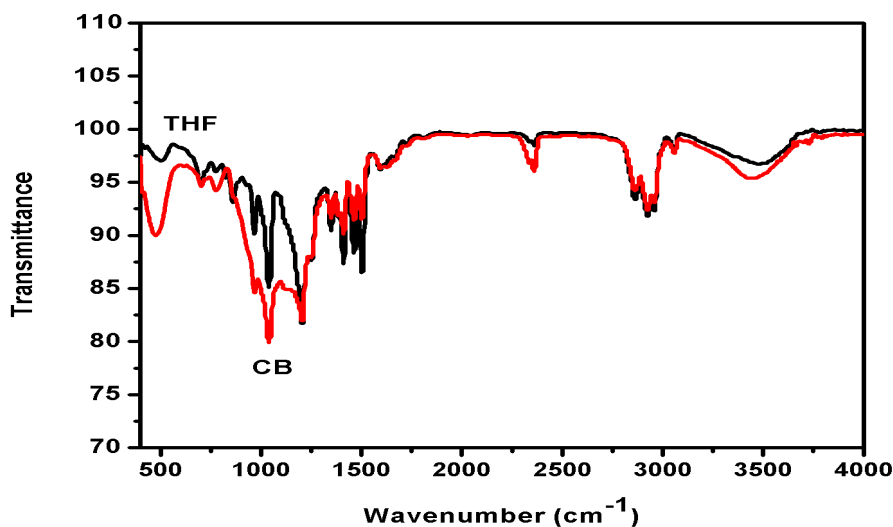


Fig. 12. FTIR spectra for MEH-PPV films based on different solvent.

Figure 13 shows that the SEM images of two different sprayed MEHPPV films based on the type of the solvent THF and CB using N_2 as an atomizing gas.

Both films are uniform and we can see that the film prepared using THF solvent, is rough compared with a polymeric film prepared using CB as a solvent.

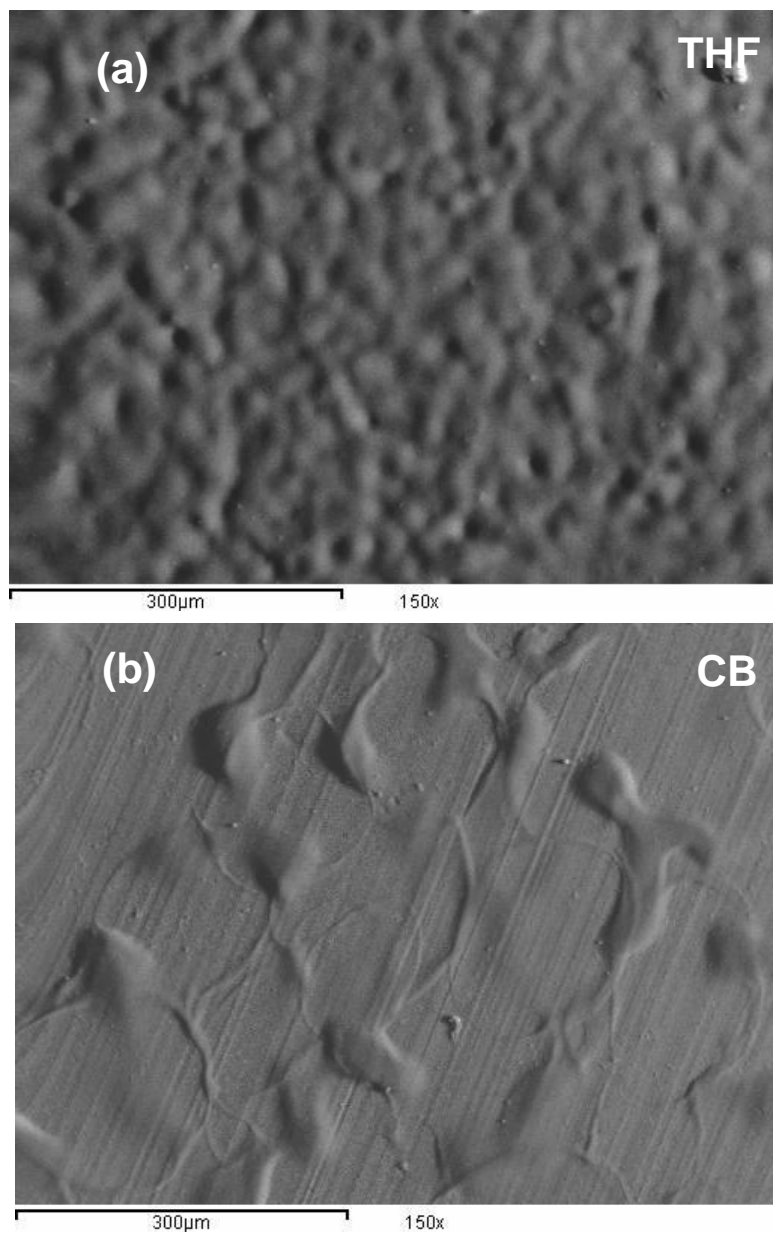


Fig. 13. SEM micrographs of MEH-PPV thin films based on different solvent.

Optical properties

The optical band gap of sprayed polymeric thin films prepared with N_2 as a carrier gas using THF and CB are around 2.05 eV and 2.07 eV, respectively as shown in Fig. 14. The change of band gap of the film prepared by THF as polymer solvent may be due to the slight change in the surface roughness of THF sample compared with CB sample. The obtained low band gap shows that the synthesized polymer may be suitable for solar cell application.

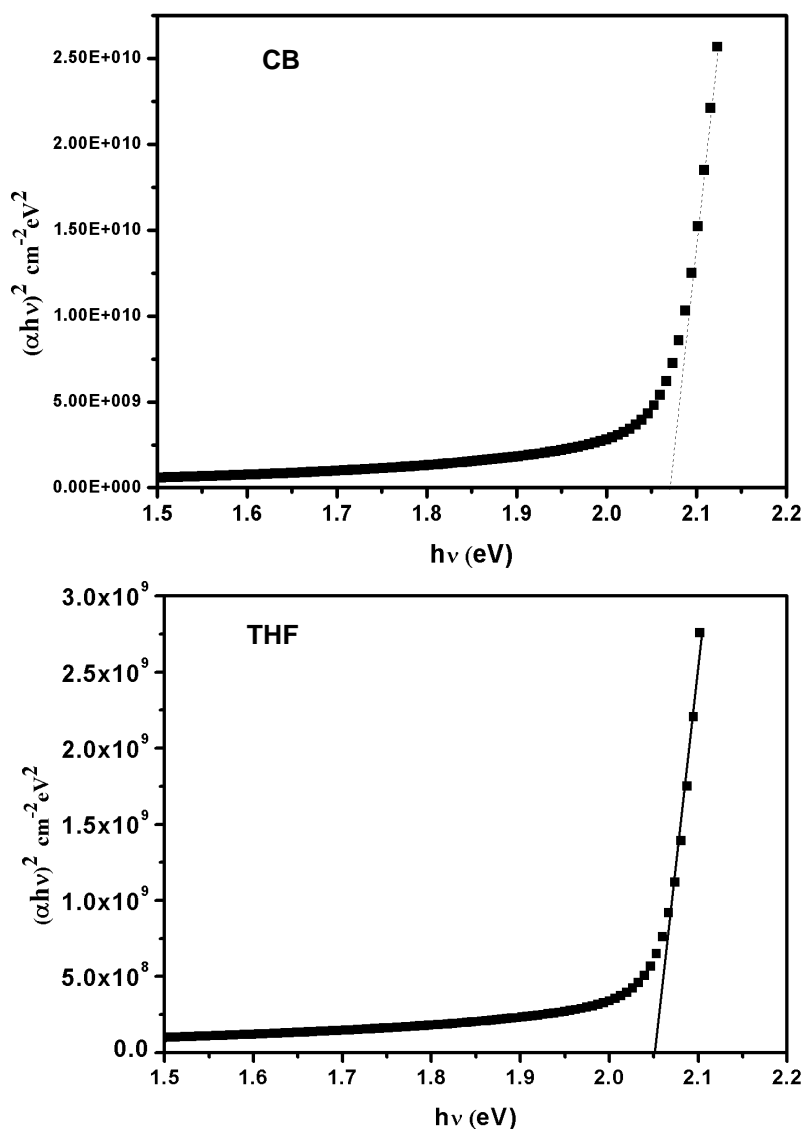


Fig. 14. $(\alpha h\nu)^2$ versus $h\nu$ of MEH-PPV thin films based on different solvent (a) CB and (b) THF.

Figure 15 shows a comparison between the PL spectra of the pristine PPV polymer spin-coated in different solvents. As shown in Fig. 15, the polymer spin-coated from THF solvent shows a higher PL intensity, compared to that spin-coated from CB solvent. Additionally, it can be seen that the polymer spin-coated from THF solvent demonstrates a peak around 592 nm and shoulder around 637 nm. While that prepared from CB solvent only shows a broad peak around 592-630 nm. The higher PL intensity observed from the THF based film compared to CB based film, may be due to the nonaromatic nature of THF (high polarity) and aromatic nature (low polarity) of CB where the emission spectra of MEH-PPV slightly red shift increase with the increase of the polarity of solvents. The improvement and red-shift of the emission in longer wavelength with the increase of concentration could be attributed to the aggregate states or inter chain excimeric states⁽²¹⁻²³⁾.

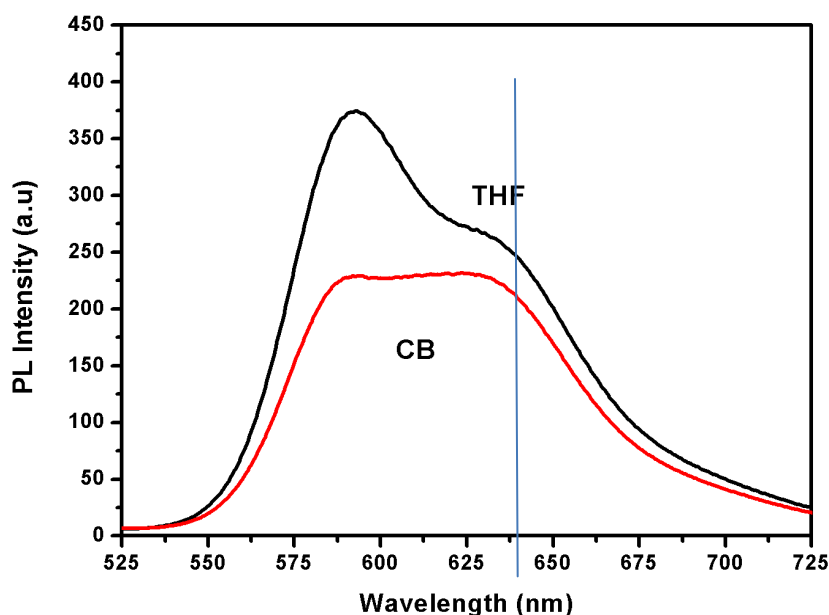


Fig. 15. PL spectra of MEH-PPV thin films based on different solvent.

Electrical properties

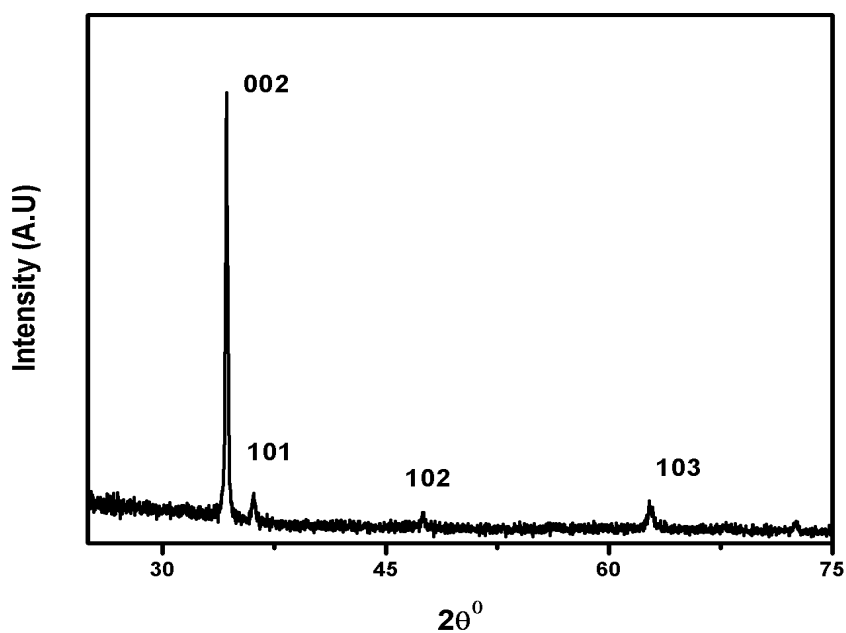
Table 1 shows some measured Hall parameters of different sprayed MEHPPV films prepared with N₂ as atomizing gas from two different solvents THF and CB. It can be seen that all the as-prepared samples are p-type where the order of resistivity of all films is same but the value of the carrier concentration density for the film prepared from THF solvent is higher than that prepared from CB solvent. The mobility is changed which may be due to the difference in the morphology of the film surface and also the slight difference in the film structure depend on the type of solvent.

TABLE 1. Summary of electrical parameters of MEH-PPV thin films based on different solvents.

Solvent	Resistivity ($\Omega\cdot\text{cm}$)	Carrier type	Bulk carrier density ($1/\text{cm}^3$)	Mobility $\text{Cm}^2/\text{v s}$
THF	2.16×10^7	p	6.45×10^{11}	2.81×10^1
CB	2.52×10^7	p	2.32×10^{11}	3.84×10^{-1}

Characterization of ZnO nanowires

Figure 16 demonstrates the XRD patterns of the ZnO nanowires array was prepared by using two-step chemical solution method on patterned fluorine tin oxide (FTO)-coated glass substrates. The XRD pattern is taken from X-ray diffractometer using $\text{CuK}\alpha$ radiation of wavelength 0.154 nm. High diffraction peaks verified greater intensity of grown nanowires. All peaks were matched by characteristic peaks of ZnO with wurtzite structure. XRD patterns indicated the growth of nanowires along c-axis. Strong diffraction peaks along (002) direction and relatively weak peaks along (101), (102) and (103) indicated vertical growth of nanowires.

**Fig. 16.** XRD of ZnO nanowires prepared by two-step method at 8 hr immersing time.

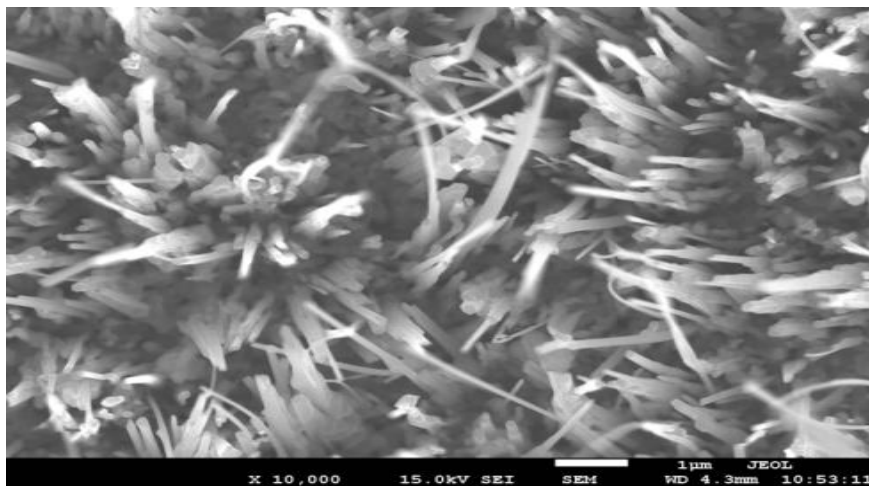


Fig. 17. FE-SEM micrographs of ZnO nanowires prepared by two-step method at 8 hr immersing time.

The general morphology of ZnO nanowires was obtained using field emission scanning electron microscopy. The SEM micrograph of the as-prepared ZnO nanowires is shown in Fig. 17. As shown ZnO nanowires were vertically well-aligned with a uniform length, diameter and distribution density, disclosing mainly aligned ZnO nanowires perpendicular to the glass substrate. The SEM observations along with XRD results suggest that the well-aligned ZnO nanowires are of good crystal orientation and morphology which makes the produced ZnO nanowires to be useful in organic-inorganic solar cell application.

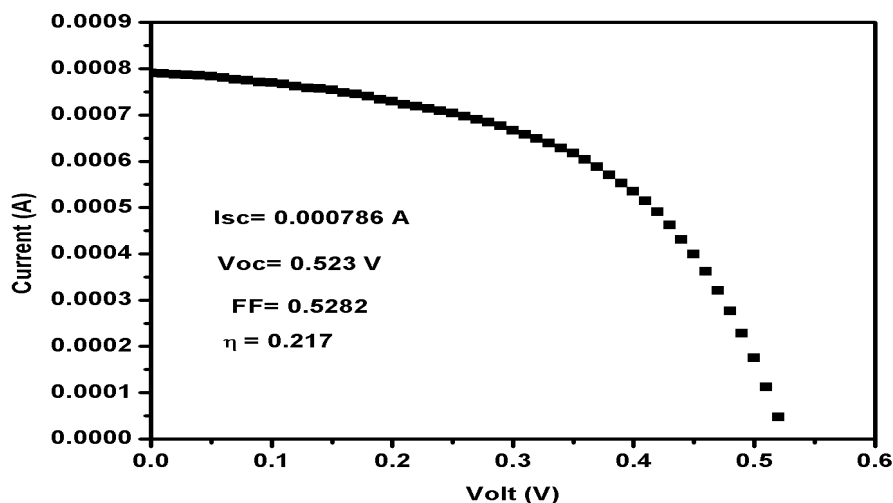


Fig.18. I-V curves of MEH-PPV solar cells based on ZnO nanowires prepared by two-step methods.

Figure 18 shows the I-V curve measurements of the solar cell constructed from MEH-PPV polymer dissolved in THF and sprayed by N₂ as atomizing gas on ZnO nanowires prepared by two steps method at 8 hr immersing time. It can be seen that the solar cell shows a fill factor of about 53%, resulting in a power conversion efficiency of $\eta=0.217$. The observed PCE displayed an improved performance compared to our previous device made from sprayed MEH-PPV polymer on sprayed ZnO nanorod/TCO glass⁽⁶⁾. This observed improvement is correlated with the improved electron transport, due to the smallest diameter of nanowires that lead to more transparent channels from ZnO materials that offer enhanced interface areas for carrier separation, improved optical light trapping compared to in case of sprayed nanorods.

Conclusion

Prepared MEH-PPV polymer shows good properties compared with the published for prepared polymer by other groups. Polymer solvent type plays an important role in controlling the properties sprayed MEH-PPV thin film. The sprayed MEH-PPV film prepared by N₂ as atomizing gas using THF as solvent shows good properties compared with that prepared with the sample used CB as the organic solvent. Finally, our solar cell efficiency based on optimum layers from polymeric thin film and ZnO nanowires shows a good result, if we compare it with the other cell that used sprayed ZnO nanorods.

Acknowledgements: This work is apart from STDF project no.1676, titled "Towards promising hybrid organic-inorganic thin film solar cell". Financial support by the Egyptian Science and Technology Fund (STDF) is gratefully acknowledged.

References

1. Yi, G.-C. Wang, C. Park, W.I., *Semicond.Sci.Technol.* **20**, S22 (2005).
2. Park, J.Y. Jung, I.O. Moon, J.H. Lee, B.-T. Kim, S.S., *J. Cryst. Growth*, 282-353 (2005).
3. Peiro, A.M. Domingo, C., Peral, J., Domenech, X., Vigil, E., Hernandez- Fenollosa, M.A., Mollar, M., , Mari, B. and Ayllon, J.A., *Thin Solid Films*, **483**, 79 (2005).
4. Li, Q. Kumar, V. Li, Y. Zhang, H. Marks, T.J. Chang, R.P.H., *Chem. Mater.*, **17**, 1001 (2005).
5. Ernst, K. Belaidi, A. Könenkamp, R. *Semicond. Sci. Technol.* **18**, 475 (2003).
6. Mahmoud, F.A. Shehata, Adel B., Hager Mohamed and Wafaa Magdy, *Journal of Advanced Materials Research*, Vol. 896 pp 489-492 (2014)
7. Huynh, W.U. Dittmer, J.J. Libby, W.C. Whiting, G.L. Alivisatos, A.P., *Advanced Functional Materials*, **13**, 73 (2003)

8. **Law, M. Greene, L.E. Johnson, J. C. Saykally, R. and Yang, P.** *Nature Materials*, **4**, 455 (2005).
9. **Baxter, J. B. and Aydil, E.S.,** *Appl. Phys. Lett.* **86**, 053114 (2005)
10. **Lévy-Clément, C. Tena-Zaera, R. Ryan, M.A. Katty, A. Hodes, G.,** *Advanced Materials*, **17**, 1512 (2005)
11. **Leschkies, K.S. Divakar, R. Basu, J. Enache-Pommer, E. Boercker, J.E. Barry Carter, C. Kortshagen, U.R. Norris, D.J. and Aydil, E.S.,** *Nano Lett.*, **7**, 1793 (2007)
12. **Ruchuan Liu,** *Materials* **7**, 2747-2771 (2014),
13. **Suzuki, Y. Hashimoto, K. and Tajima, K.,** *Macromolecules*, **40**(18), 6521–6528 (2007).
14. **Neef, C. J. and Ferraris, J.P.,** *Macromolecules*, **33**,(7), 2311–2314(2000).
15. **Norlida Kamarulzaman, Nor Diyana Abdul Aziz, Ri Hanum Yahaya Subban, Ahmad Sazali Hamzah, Azni Zain Ahmed, Zurina Osman, Roshidah Rusdi, Norashikin Kamarudin , Nor SaliyanaJumali and Zurina Shaameri.** *3rd International Symposium & Exhibition in Sustainable Energy & Environment*, 1-3 June 2011, Melaka, Malaysia
16. **Habibur Rahman, M. Hsin-Lung Chen, Show-An Chen and Peter P.J.,** *Chu, Journal of the Chinese Chemical Society*, **57**, 490-495 (2010)
17. **Liu, J., Guo, T.F., Shi, Y. and Yang, Y.,** *J. Appl. Phy*, **89**, 3668 (2001).
18. **. Liu, J, Guo, T.F. and Yan ,Y.,** *J. Appl. Phy.* **91**, 1595 (2002).
19. **Lee, T.W. and Park, O.O.,** *Curr. App. Phy.* **9**, 1315 (2009)
20. **Souza, A.A., Cassiello, R.F., Plivelic, T.S., Mantovani, G.L., Faria, G.C., Atvars, T.D.Z., Torriani, I.L., Bonagamba, T.J. and deAzivedo, T.R. ,** *Eur. Polym. J.* **44**, 4063 (2008).
21. **Harrison, N.T. Baigent, D.R. Samuel, I.D.W. Friend, R. H.,** *PHYSICAL REVIEW B*, **53**, 15815 (1996).
22. **Zheng, M., Bai, F. and Zhu, D.,** *Journal of Photochemistry and Photobiology A: Chemistry* **116**, 143-145 (1998)
23. **Tetsuo Soga,** *Nanostructured Materials for Solar Energy Conversion*, Elsevier, Netherland, 290 (2006).

Received 24/8/2016 ;
accepted 17/10/2016)

تخليق وتوصيف بوليمر الفينيلين فاينيلدين وتطبيقه في الخلايا الشمسية

فوزي عبد الحميد محمود^{1,2}، ياسر عاصم^{2,3} وعادل بسيوني شحاته⁴ وديفيد موتونج⁵
¹قسم جوامد الفيزياء، ²مركز التميز العلمي بمجموعة الخلايا الشمسية، ³قسم البوليمرات
والمخضبات-المركز القومي للبحوث، ⁴المعهد القومي للمعايرة و⁵المركز القومي للمواد
النانومترية بجوهانسبرج-جنوب افريقيا.

في هذا البحث تم تحضير بوليمر Poly [2-methoxy-5-(2'-ethylhexyloxy)-1,4-phenylene vinylene] (MEH-PPV) بطريقة Gilch. و تم تأكيد تكوين البوليمر باستخدام طيف الرنين المغناطيسي النووي (NMR) لنواة كل من ¹³C و ¹H بالاضافة الى طيف الاشعة تحت الحمراء (FTIR). و تم دراسة الخصائص الحرارية للبوليمر باستخدام (TGA / DSC) وقد وتم حل عينتين من البوليمر في اثنين من المذيبات العضوية المختلفة (THF و كلور بنزين CB) و تم تكوين فيلم رقيق على كل الزجاج و KBR عند 150 درجة مئوية. و تم تكوين فيلم من البوليمر الذائب في THF على أسلاك أكسيد الزنك. و قد أظهرت الخلايا الشمسية التي شيدت أداء أفضل مقارنة مع الخلايا السابقة التي تستخدم أكسيد الزنك على هيئة قضبان نانومترية.